Inorg. Chem. **2009**, *48*, 2526−2533

$Eu_3Co_2In_{15}$ and KM_2In_9 (M = Co, Ni): 3D Frameworks Based on Transition Metal Centered In_9 Clusters

Xiao-Wu Lei,[†,‡] Guo-Hua Zhong,[†] Long-Hua Li,[†,‡] Chun-Li Hu,[†] Min-Jie Li,[†,‡] and Jiang-Gao Mao*[,†]

State Key Laboratory of Structural Chemistry, Fujian Institute of Research on the Structure of Matter, Chinese Academy of Sciences, Fuzhou 350002, P. R. China, and Graduate School of the Chinese Academy of Sciences, Beijing 100039, P. R. China

Received October 16, 2008

The title three compounds have been synthesized by solid state reactions at high temperatures, with excess indium as flux, and structurally characterized by single-crystal X-ray diffraction studies. $Eu_3Co_2In_{15}$ forms a new structure type and crystallizes in the tetragonal space group *P*4/*mbm* (No. 127), whereas KM_2In_9 (M = Co, Ni) in the $BaFe_2Al_9$ type crystallizes in the hexagonal space group *P*6/*mmm* (No. 191). Their structures all feature a three-dimensional anionic framework based on 1D $[MIn_6]$ single cluster chains composed of face-sharing $[MIn_9]$ clusters. In $Eu_3Co_2In_{15}$, two adjacent $[CoIn_6]$ single cluster chains form a $[Co_2In_{11}]$ double cluster chain via corner-sharing In atoms as well as In−In bonds; the latter chains are further interconnected by additional indium atoms via In−In bonds into a complicated 3D framework, forming two types of tunnels along the *c*-axis, which are filled by the europium atoms. In KM_2In_9, the $[MIn_6]$ single cluster chains are directly interconnected via corner sharing and exo In−In bonds into a 3D framework with the K^+ ions encapsulated in the 1D tunnels along the *c*-axis. Band structure calculations of three compounds based on density functional theory methods indicate that all three compounds are metallic.

Introduction

Polar intermetallics of the indium element with one or more of the electropositive alkali or alkaline earth metals have been investigated intensively in the past several decades because of their remarkable structural diversity, novel chemical bonding, and intriguing physical properties.[1−11] A number of binary phases with 3D indium networks have been reported, such as $AeIn_2$ (Ae = Ca, Sr, Ba),[4] Sr_3In_5,[5] $SrIn_4$, and Sr_3In_{11}.[6] Similar to gallium phases, indium generally forms extended anionic cluster frameworks, with a few examples of discrete clusters.[7−11] A few of these phases follow the Zintl−Klemn electron count rules, whereas the chemical bonding and structures of many other compounds are much more complicated.[1,12,13]

* To whom correspondence should be addressed. E-mail: mjg@fjirsm.ac.cn.
† Fujian Institute of Research on the Structure of Matter, Chinese Academy of Sciences.
‡ Graduate School of the Chinese Academy of Sciences.

(1) (a) Corbett, J. D. In *Chemistry, Structure and Bonding of Zintl Phases and Ions*; Kauzlarich, S. M., Ed.; VCH Publishers: New York, 1996; p 139. (b) Miller, G. J. In *Chemistry, Structure and Bonding of Zintl Phases and Ions*; Kauzlarich, S. M., Ed.; VCH Publishers: New York, 1996; p 1. (c) Eisenmann, B.; Cordier, G. In *Chemistry, Structure and Bonding of Zintl Phases and Ions*; Kauzlarich, S. M., Ed.; VCH Publishers: New York, 1996; p 61 and references therein.
(2) Belin, C.; Tillard-Charbonnel, M. *Prog. Solid State Chem.* **1993**, *22*, 59.
(3) Belin, C.; Tillard-Charbonnel, M. *Coord. Chem. Rev.* **1998**, *180*, 529.
(4) (a) Nuspl, G.; Polborn, K.; Evers, J.; Landrum, G. A.; Hoffmann, R. *Inorg. Chem.* **1996**, *35*, 6922. (b) Wendorff, M.; Röhr, C. *Z. Anorg. Allg. Chem.* **2005**, *631*, 338. (c) Björling, T.; Noréus, D.; Häussermann, U. *J. Am. Chem. Soc.* **2006**, *128*, 817.
(5) Seo, D. K.; Corbett, J. D. *J. Am. Chem. Soc.* **2001**, *123*, 4512.
(6) (a) Seo, D. K.; Corbett, J. D. *J. Am. Chem. Soc.* **2000**, *122*, 9621. (b) Amerioun, S.; Häussermann, U. *Inorg. Chem.* **2003**, *42*, 7782. (c) Mao, J.-G.; Guloy, A. M. *J. Alloys Compd.* **2004**, *363*, 143.
(7) (a) Li, B.; Corbett, J. D. *J. Am. Chem. Soc.* **2005**, *127*, 926. (b) Burdett, J. K.; Canadell, E. *J. Am. Chem. Soc.* **1990**, *112*, 7207.
(8) (a) Sevov, S. C.; Corbett, J. D. *Inorg. Chem.* **1991**, *30*, 4875. (b) Li, B.; Corbett, J. D. *Inorg. Chem.* **2003**, *42*, 8768. (c) Cordier, G.; Müller, V. *Z. Kristallogr.* **1993**, *205*, 353.
(9) (a) Sevov, S. C.; Corbett, J. D. *Inorg. Chem.* **1992**, *31*, 1895. (b) Sevov, S. C.; Corbett, J. D. *J. Solid State Chem.* **1993**, *103*, 114.
(10) (a) Sevov, S. C.; Corbett, J. D. *Inorg. Chem.* **1993**, *32*, 1612. (b) Mao, J.-G.; Goodey, J.; Guloy, A. M. *Inorg. Chem.* **2004**, *43*, 282. (c) Li, B.; Corbett, J. D. *Inorg. Chem.* **2002**, *41*, 3944.
(11) (a) Sun, Z.-M.; Mao, J.-G.; Pan, D.-C. *Inorg. Chem.* **2005**, *44*, 6545. (b) Li, B.; Corbett, J. D. *Inorg. Chem.* **2007**, *46*, 2237. (c) Chi, L.-S.; Corbett, J. D. *Inorg. Chem.* **2001**, *40*, 3596. (d) Li, B.; Corbett, J. D. *Inorg. Chem.* **2006**, *45*, 3861.
(12) (a) Nesper, R. *Angew. Chem., Int. Ed. Engl.* **1991**, *30*, 789. (b) Nesper, R. *Prog. Solid State Chem.* **1990**, *20*, 1.

10.1021/ic8019765 CCC: $40.75
Published on Web 02/09/2009

In recent years, systematic research efforts in this area have led to the extension of these systems to include all lanthanide elements, as well as most of the transition metals. Such design strategy led to diverse structures with unique indium networks.[14−19] For example, the ternary compounds $CaMIn_2$, $SrMIn_2$, and $BaMIn_2$ (M = Rh, Pd, Pt, Ir)[14] can be considered as transition metal filled variants of the Zintl phases $CaIn_2$, $SrIn_2$, and $BaIn_2$, respectively.[4] With a higher indium content, indides such as $REPtIn_3$ (RE = La−Nd, Sm), $REMIn_4$ (M = Rh, Ni, Pd, Pt), and $EuRh_2In_8$ with various 3D framework structures have been reported.[15,16] The most indium rich compounds $REMIn_5$ and RE_2MIn_8 (M = Co, Rh, Ir) of the homologous RE_nMIn_{3n+2} (n = 1, 2, ∞) series have attracted considerable interest in recent years because of their outstanding physical properties.[17] For example, $CeMIn_5$ is in a special class of heavy fermion materials which show magnetic ordering and unconventional superconductivity at low temperature. It should be noted that the common structural motifs are distorted body centered cube (bcc)-like indium cubes for most of these indides, which somehow resemble the structure of elemental indium. Using bcc-like indium cubes as fundamental building blocks, different structures can be constructed via diverse condensation schemes. Similar structural motifs can also be found in a number of ternary gallium phases.[20] In addition, a variety of A−M−In (A is an alkali metal) ternary phases have also been prepared and their structures elucidated, such as K_8MIn_{10} (M = Hg, Zn), $K_{10}MIn_{10}$ (M = Ni, Pd, Pt), Na_3MIn_2 (M = Au, Ag), AAu_4In_2 (A = K, Rb), $K_{34}Zn_{13.05}In_{89.95}$, and so forth.[21]

The introduction of the transition metal into the above A−In systems can dramatically change the structure and physical properties of the compounds because of the formation of M−In bonds.[14,22] We are especially interested in the syntheses and structures of the ternary Eu−Co−In phases, but so far, none of them have been reported. Our exploratory studies led to the first europium cobalt indide, $Eu_3Co_2In_{15}$. Its structure features a 3D framework based on the $[Co_2In_{11}]$ double cluster chains from $[CoIn_9]$ clusters. The replacement of lanthanide metal by potassium metal led to the discovery of two new polar intermetallics, KM_2In_9 (M = Co, Ni). Their structures also feature a 3D framework based on the similar $[MIn_9]$ clusters. Herein, we report their syntheses, single-crystal structures, and band structures.

Experimental Section

Materials and Instrumentation. All manipulations were performed within an argon-filled glovebox with a moisture level below 1 ppm. All chemicals were used as received: potassium blocks (Shanghai fourth chemical reagent company, 99.99%), europium bricks (Acros, 99.99%), cobalt and nickel powder (Shanghai fourth chemical reagent company, 99.99%), and indium granules (Acros, 99.999%). Elemental analyses for K, Eu, Co, Ni, and In were performed on a JSM-6700F scanning electron microscope equipped with an energy dispersive X-ray spectroscope (EDS, Oxford INCA). Data were acquired with an accelerating voltage of 20 kV and scanning electron microscopy of 40°. X-ray diffraction (XRD) powder patterns were collected at room temperature on an X'Pert-Pro diffractometer using Cu Kα radiation (λ = 1.5406 Å) in the 2θ range of 5−85° with a step size of 0.04° and 10 s/step counting time. The generator voltage was 45 kV, and the tube current was 40 mA. The data analysis was performed using the JADE 5.0 software package.

Preparation of $Eu_3Co_2In_{15}$. Single crystals of $Eu_3Co_2In_{15}$ were initially obtained from a mixture of Eu, Co, and In metals in a molar ratio of 1:1:10, and the large excess of indium metal was used as the flux. The mixture was loaded into a tantalum tube, which was subsequently arc-welded under an argon atmosphere and sealed in a quartz tube under vacuum (~10^{-4} Torr). The quartz tube was put into a high-temperature furnace, allowed to react at 980 °C for 6 days, and annealed at 650 °C for 7 days. Then it was allowed to cool at a rate of 0.1 °C/min to room temperature. Prism-shaped silvery white single crystals of $Eu_3Co_2In_{15}$ were selected from the reaction products. Microprobe elemental analyses on several single crystals indicated the presence of Eu, Co, and In elements in a molar ratio of 2.8(2):1.9(1):15.4(9), which was in agreement with the results from single crystal XRD studies. The compound is stable

(13) (a) Zintl, E. *Angew. Chem.* **1939**, *52*, 1. (b) Klemm, W.; Busmann, E. *Z. Anorg. Allg. Chem.* **1963**, *319*, 297. (c) Wade, K. *Adv. Inorg. Chem. Radiochem.* **1976**, *18*, 1.
(14) (a) Hoffmann, R.-D.; Pöttgen, R.; Landrum, G. A.; Dronskowski, R.; Künnen, B.; Kotzyba, G. *Z. Anorg. Allg. Chem.* **1999**, *625*, 789. (b) Hoffmann, R.-D.; Rodewald, U. C.; Pöttgen, R. *Z. Naturforsch., B: Chem. Sci.* **1999**, *54*, 38. (c) Hoffmann, R.-D.; Pöttgen, R. *Chem.−Eur. J.* **2001**, *7*, 382.
(15) Galadzhun, Y. V.; Pöttgen, R. *Z. Anorg. Allg. Chem.* **1999**, *625*, 481.
(16) (a) Hoffmann, R.-D.; Pöttgen, R.; Zaremba, V. I.; Kalychak, Y. M. *Z. Naturforsch.* **2000**, *55B*, 834. (b) Pöttgen, R.; Müllmann, R.; Mosel, B. D.; Eckert, H. *J. Mater. Chem.* **1996**, *6* (5), 801. (c) Pöttgen, R.; Kussmann, D. *Z. Anorg. Allg. Chem.* **2001**, *627*, 55.
(17) (a) Williams, W. M.; Pham, L.; MaQuilon, S.; Moldovan, M.; Fisk, Z.; Young, D. P.; Chan, J. Y. *Inorg. Chem.* **2006**, *45*, 4637. (b) Park, T.; Ronning, F.; Yuan, H. Q.; Salamon, M. B.; Movshovich, R.; Sarrao, J. L.; Thompson, J. D. *Nature* **2006**, *440*, 65. (c) Macaluso, R. T.; Sarrao, J. L.; Moreno, N. O.; Pagliuso, P. G.; Thompson, J. D.; Fronczek, F. R.; Hundley, M. F.; Malinowski, A.; Chan, J. Y. *Chem. Mater.* **2003**, *15*, 1394. (d) Shaginyan, V. R.; Stephanovich, V. A.; Kirichenko, E. V. *J. Alloys Compd.* **2007**, *442*, 119.
(18) (a) Kalychak, Y. M.; Zaremba, V. I.; Galadzhun, Y. V.; Miliyanchuk, K. Y.; Hoffmann, R.-D.; Pöttgen, R. *Chem.−Eur. J.* **2001**, *7*, 5343. (b) Zhao, J.-T.; Corbett, J. D. *Inorg. Chem.* **1995**, *34*, 378. (c) Kalychak, Y. M. *J. Alloys Compd.* **1999**, *291*, 80. (d) Hlukhyy, V.; Zaremba, V. I.; Kalychak, Y. M.; Pöttgen, R. *J. Solid State Chem.* **2004**, *177*, 1359. (e) Pöttgen, R.; Hoffmann, R.-D.; Kremer, R. K.; Schnelle, W. *J. Solid State Chem.* **1999**, *142*, 180.
(19) (a) Tkachuk, A. V.; Mar, A. *J. Solid State Chem.* **2007**, *180*, 2298. (b) Hoffmann, R.-D.; Pöttgen, R. *Chem.−Eur. J.* **2000**, *6*, 600. (c) Tursina, A. I.; Kurenbaeva, Z. M.; Gribanov, A. V.; Noël, H.; Roisnel, T.; Seropegin, Y. D. *J. Alloys Compd.* **2007**, *442*, 100. (d) Zaremba, V. I.; Rodewald, U. C.; Lukachuk, M.; Dubenskiy, V. P.; Heying, B.; Katoh, K.; Niide, Y.; Ochiai, A.; Pöttgen, R. *Monatsh. Chem.* **2006**, *137*, 249. (e) Zaremba, V. I.; Rodewald, U. C.; Lukachuk, M.; Dubenskiy, V. P.; Heying, B.; Katoh, K.; Niide, Y.; Ochiai, A.; Pöttgen, R. *Monatsh. Chem.* **2006**, *137*, 249.
(20) Jia, Y.-Z.; Belin, C.; Tillard, M.; Lacroix-Orio, L.; Zitoun, D.; Feng, G.-H. *Inorg. Chem.* **2007**, *46*, 4177.
(21) (a) Sevov, S. C.; Ostenson, J. E.; Corbett, J. D. *J. Alloys Compd.* **1993**, *202*, 289. (b) Sevov, S. C.; Corbett, J. D. *Inorg. Chem.* **1993**, *32*, 1059. (c) Sevov, S. C.; Corbett, J. D. *J. Am. Chem. Soc.* **1993**, *115*, 9089. (d) Li, B.; Corbett, J. D. *Inorg. Chem.* **2005**, *44*, 6515. (e) Li, B.; Corbett, J. D. *Inorg. Chem.* **2006**, *45*, 8958. (f) Li, B.; Corbett, J. D. *J. Am. Chem. Soc.* **2006**, *128*, 12392.
(22) (a) Hoffmann, R.-D.; Pöttgen, R. *Z. Anorg. Allg. Chem.* **2000**, *626*, 28. (b) Hoffmann, R.-D.; Kussmann, D.; Rodewald, U. C.; Pöttgen, R.; Rosenhahn, C.; Mosel, D. *Z. Naturforsch., B: Chem. Sci.* **1999**, *54*, 709.
(23) (a) *CrystalClear*, Version 1.3.5; Rigaku Corp.: Woodlands, TX, 1999. (b) Sheldrick, G. M. *SHELXTL, Crystallographic Software Package*, Version 5.1; Bruker-Axs: Madison, WI, 1998.

in moist air for several weeks. After the structure and the composition analyses, many efforts were subsequently made to prepare a single phase of $Eu_3Co_2In_{15}$. The reactions were carried out with a stoichiometric mixture of the elements. The samples were heated at 980 °C for 2 days and then quenched in water. Then, the reaction product was grinded, sealed, and annealed again at 600 °C for 15 days. XRD powder patterns of the resultant products revealed the presence of impurity phase $EuIn_4$ (*C*2/*m*) in addition to $Eu_3Co_2In_{15}$ (87%) as the major phase. Attempts were also made to prepare the Sr analogue of $Eu_3Co_2In_{15}$ by using similar conditions to those of $Eu_3Co_2In_{15}$. XRD powder and semiquantitative microprobe elemental analysis for the products revealed the presence of $SrIn_4$ (*C*2/*m*) as the major phase but showed no indication of $Sr_3Co_2In_{15}$. Attempts to prepare the analogues of other lanthanide elements, such as Yb, were also unsuccessful.

Preparation of KM_2In_9 (M = Co, Ni). Single crystals of KCo_2In_9 and KNi_2In_9 were initially obtained from a mixture of K, Co (or Ni), and In elements in a molar ratio of 9:1:9. Their synthetic procedure is similar to that of $Eu_3Co_2In_{15}$. The samples were heated to 800 °C over 3 days and held at that temperature for additional 6 days. It was then cooled to 500 °C and held at this temperature for 7 days, and then the samples were cooled to room temperature in 5 days. Prism-shaped gray and silvery white single crystals of KCo_2In_9 and KNi_2In_9, respectively, were found in the reaction products. Microprobe analyses on several single crystals of KCo_2In_9 and KNi_2In_9 gave molar ratios of 0.9(2):1.9(1):9.2(5) (K:Co:In) for KCo_2In_9 and 0.9(5):1.8(5):9.2(4) (K:Ni:In) for KNi_2In_9, respectively, which were in good agreements with those from the structural refinements. Both compounds are air and hydrosphere sensitive. After proper structural analyses, attempts were made to prepare the single phase of KM_2In_9 through the solid state reactions of the stoichiometric mixtures of the pure elements in Ta tubes at different temperatures (650, 700, 750, 800, and 850 °C, respectively, for each individual reaction) for 10 days, which cooled at a rate of 0.1 °C/min to room temperature. However, XRD powder patterns of the resultant products always indicate the presence of the impurity phases, such as K_8In_{11} ($R\bar{3}c$), as well as other unidentified compounds. The high yields of ~60% and ~70% for KCo_2In_9 and KNi_2In_9, respectively, were obtained by reactions at 650 °C.

Crystal Structure Determination. Single crystals of $Eu_3Co_2In_{15}$, KCo_2In_9, and KNi_2In_9 were selected from the reaction products and sealed into thin-walled glass capillaries within the glovebox. Data collections for both compounds were performed on a Rigaku Mercury CCD (Mo Kα radiation, graphite monochromator) at 293(2) K. All three data sets were corrected for Lorentz factor, polarization, air absorption, and absorption because of variations in the path length through the detector faceplate. Absorption corrections based on the multiscan method were also applied.[23a]

All three structures were solved using direct methods (SHELXTL) and refined by least-squares methods with atomic coordinates and anisotropic thermal parameters.[23b] For $Eu_3Co_2In_{15}$, inspection of the systematic absences for the full data set indicated the possible space group to be *P*4/*mbm* (No. 127), $P\bar{4}b2$ (No. 117), or *P*4*bm* (No. 100). The mean $|E^2 - 1|$ value of 0.976 was suggestive of a centrosymmetric space group; hence, *P*4/*mbm* was selected and used for structural refinements. KM_2In_9 (M = Co, Ni) crystallized in the hexagonal space group *P*6/*mmm* (No. 191) on the basis of systematic absences and *E*-value statistics. Site occupancy refinements for the three compounds indicated that all sites were fully occupied. Final difference Fourier maps showed featureless residual peaks of 1.27 e·Å^3 (0.84 Å from the Eu(2) atom) and −1.49 e·Å^3 (0.74 Å from the In(3) atom) for $Eu_3Co_2In_{15}$; 0.36 e·Å^3 (0.00 Å from the K(1) atom) and −0.67 e·Å^3 (0.80 Å from the In(2) atom) for KCo_2In_9; and 0.52 e·Å^3 (0.76 Å from the In(1) atom) and −0.98 e·Å^3 (0.46 Å from the Ni(1) atom) for KNi_2In_9, respectively. Data collection and refinement parameters are summarized in Table 1. Atomic coordinates and important bond lengths are listed in Tables 2 and 3, respectively. More details about crystallographic studies and atomic displacement parameters are given in the Supporting Information.

Table 1. Crystal Data and Structure Refinements for Compounds $Eu_3Co_2In_{15}$ and KM_2In_9 (M = Co, Ni)

chemical formula	$Eu_3Co_2In_{15}$	KCo_2In_9	KNi_2In_9
fw	2296.04	1190.34	1189.90
space group	*P*4/*mbm* (No. 127)	*P*6/*mmm* (No. 191)	*P*6/*mmm* (No. 191)
a, Å	14.7890(4)	8.7915(7)	8.7915(7)
c, Å	4.3945(2)	4.2364(4)	4.2380(5)
V (Å^3)	961.14(6)	283.57(4)	283.67(5)
Z	2	1	1
D_{calcd} (g cm^{-3})	7.934	6.971	6.965
temp (K)	293(2)	293(2)	293(2)
μ (mm^{-1})	28.855	21.067	21.454
GOF on F^2	1.111	1.271	1.259
R1, wR2 ($I > 2\sigma(I)$)[a]	0.0177, 0.0397	0.0107, 0.0261	0.0118, 0.0285
R1, wR2 (all data)	0.0210, 0.0405	0.0107, 0.0261	0.0118, 0.0285

[a] $R1 = \sum||F_o| - |F_c||/\sum|F_o|$, $wR2 = \{\sum w[(F_o)^2 - (F_c)^2]^2/\sum w[(F_o)^2]^2\}^{1/2}$.

Table 2. Atomic Coordinates and Equivalent Isotropic Displacement Parameters (Å^2 × 10^3) for $Eu_3Co_2In_{15}$ and KM_2In_9 (M = Co, Ni)

atom	Wyckoff	*x*	*y*	*z*	*U*(eq)[a]
		$Eu_3Co_2In_{15}$			
Eu(1)	2b	0	0	1/2	7(1)
Eu(2)	4h	0.3246(1)	0.1754(1)	1/2	14(1)
Co(1)	4h	0.1212(1)	0.3788(1)	1/2	10(1)
In(1)	2c	0	1/2	1/2	10(1)
In(2)	4g	0.2042(1)	0.2958(1)	0	9(1)
In(3)	8j	0.0692(1)	0.2099(1)	1/2	13(1)
In(4)	8i	0.1519(1)	0.4982(1)	0	9(1)
In(5)	8i	0.1551(1)	0.0821(1)	0	14(1)
		KCo_2In_9			
K(1)	1a	0	0	0	24(1)
Co(1)	2c	1/3	2/3	0	8(1)
In(1)	6m	0.2084(1)	0.4168(1)	1/2	12(1)
In(2)	3f	0	1/2	0	14(1)
		KNi_2In_9			
K(1)	1a	0	0	0	25(1)
Ni(1)	2c	1/3	2/3	0	11(1)
In(1)	6m	0.2084(1)	0.4167(1)	1/2	12(1)
In(2)	3f	0	1/2	0	14(1)

[a] *U*(eq) is defined as one-third of the trace of the orthogonalized U_{ij} tensor.

Table 3. Selected Bond Lengths (Å) for Compounds $Eu_3Co_2In_{15}$ and KM_2In_9 (M = Co, Ni)

	$Eu_3Co_2In_{15}$		
Eu(1)−In(3)	3.2679(5) × 4	In(1)−In(4)	3.1419(4) × 8
Eu(1)−In(5)	3.4005(4) × 5	In(2)−In(3)	3.2293(4) × 4
Eu(1)−In(5)	3.4004(4) × 3	In(2)−In(4)	3.0920(7) × 2
Eu(2)−In(2)	3.3416(6) × 2	In(2)−In(5)	3.2431(6) × 2
Eu(2)−In(4)	3.4378(4) × 4	In(3)−In(4)	3.1633(5) × 2
Eu(2)−In(5)	3.6076(4) × 4	In(3)−In(5)	3.1641(5) × 2
Eu(2)−In(1)	3.6691(5)	In(3)−In(5)	3.2389(5) × 2
Co(1)−In(1)	2.536(1)	In(4)−In(4)	3.1385(9)
Co(1)−In(2)	2.7997(8) × 2	In(4)−In(4)	3.2131(9)
Co(1)−In(3)	2.6138(7) × 2	In(4)−In(5)	3.1127(7)
Co(1)−In(4)	2.8555(5) × 4		
	KCo_2In_9		
K(1)−In(1)	3.8153(3) × 12	In(1)−In(1)	3.1733(4) × 2
Co(1)−In(1)	2.8471(3) × 6	In(1)−In(1)	3.2952(6) × 2
Co(1)−In(2)	2.5379(2) × 3	In(1)−In(2)	3.1175(2) × 4
	KNi_2In_9		
K(1)−In(1)	3.8155(4) × 12	In(1)−In(1)	3.1730(5) × 2
Ni(1)−In(1)	2.8480(3) × 6	In(1)−In(1)	3.2958(7) × 2
Ni(1)−In(2)	2.5379(2) × 3	In(1)−In(2)	3.1181(2) × 4

Computational Details. Ab initio electronic structure calculations for the three compounds were performed with both the full-potential linearized augumented plane wave plus the local basis (FPLAPW + lo) method (WIEN2K) and the tight-binding linear muffin-tin orbital (TB-LMTO-ASA) methods to understand the chemical bonding of the three compounds.

WIEN2K. The WIEN2K program is based on the density functional theory and the highly accurate full-potential linearized augumented plane wave plus the local basis method, using the general gradient approximation (GGA-PBE) to treat the exchange and correlation potential.[24] The calculation sets were based on the primitive cell for both compounds ($Eu_3Co_2In_{15}$, $Z = 2$; KM_2In_9, $Z = 1$). To obtain as precise results as possible, we expanded the basis function up to $R_{MT} \times K_{MAX} = 7$, where R_{MT} is the smallest muffin-tin spherical radius present in the system and K_{MAX} is the maximum modulus for the reciprocal lattice vector. We adopted the values of 2.5, 2.5, 2.5, and 2.24 Å for K, Eu, Co (Ni), and In atoms, respectively, as the R_{MT} radii. The valence states set included the 4s orbitals for K; 4f, 5d, and 6s orbitals for Eu; 3d and 4s orbitals for Co (Ni); and 5s and 5p orbitals for In atoms, respectively, which were expanded using the basis functions. Convergence of the self-consistent iterations was performed inside the reduced Brillouin Zone to be within 0.0001 cc with a cutoff energy of −8.0 Ry between the valence and the core states. We calculated the total energy and magnetic moments with the 100, 200, and 500 *k*-points for all compounds, and the results suggested that the calculated results did not change much from 100 to 500 *k*-points. So in this study, we used the 100 *k*-point in the complete Brillouin zone, and the Brillouin zone integration was carried out with a modified tetrahedron method.[25] The Fermi level was selected as the energy reference ($E_F = 0$ eV).

Stuttgart LMTO Program. This program follows the TB-LMTO method in the local density and atomic sphere (ASA) approximations. Interstitial spheres are introduced in the last to achieve space filling. The ASA radii as well as the positions and radii of additional empty spheres are calculated automatically. The basis set included the 6s, 6p, 5d, and 4f orbitals for Eu; 4s, 4p, and 3d orbitals for K; 4s, 4p, 3d, and 3f orbitals for Co and Ni; and 5s, 5p, 4d, and 4f orbitals for In atoms. The K 4p, Eu 6p, Co (Ni) 3f, and In 4d, 4f orbitals were treated with the down-folding technique.[27] In both cases, the *k*-space integrations were performed by the tetrahedron method.[25] The Fermi level was selected as the energy reference ($E_F = 0$ eV).

Results and Discussion

Exploratory syntheses in ternary RE (or A)−M−In systems led to three novel intermetallic phases, namely, $Eu_3Co_2In_{15}$ and KM_2In_9 (M = Co, Ni). Their structures all feature a 3D network based on 1D $[MIn_6]$ single cluster chains based on face-sharing transition metal centered $[In_9]$ clusters. It should be mentioned that these "clusters" are not real ones; the terms are used just for convenience to describe their structures.

The structure of $Eu_3Co_2In_{15}$ features a novel 3D anionic network in which the $[Co_2In_{11}]$ double chains are further bridged by additional indium atoms via In−In bonds, forming tunnels of five- and eight-membered rings along the *c*-axis (Figure 1a). There are two Eu, one Co, and five In atoms in the asymmetric unit of $Eu_3Co_2In_{15}$. Four In(4) and two In(2) atoms form a trigonal prism; its three rectangular faces are capped by one In(1) and two In(3) atoms to form an $[In_9]$ cluster. The In−In bonds are in the range of 3.0920(7)−3.2293(4) Å, which is slightly longer than the sum of the covalent radii of 2.89 Å[28] and comparable to those reported in other indium phases such as $EuRhIn_2$ and $EuRh_2In_8$.[14−21] However, they are slightly shorter than those in the tetragonal body-centered structure of elemental indium (*I4/mmm*), where each indium atom has four nearest neighbors at 3.251 Å and eight further neighbors at 3.377 Å.[29] The cobalt atom is located at the center of the $[In_9]$ cage with the Co−In distances in the range of 2.536(1)−2.8555(5) Å, which is very close to the sum of the covalent radii of 2.672 Å[28] and those reported in Co_4In_{12} ($P4_2/mnm$), Ce_2CoIn_8, $LaCoIn_5$, and $YbCoIn_5$.[30] The relatively short Co−In distances are indicative of strong covalent Co−In bonding. Similar transition metal centered clusters have also been reported for $[CuSn_9]^{3-}$ and $[CuPb_9]^{3-}$ in $[K([2,2,2]crypt)]_3[Cu@E_9](dmf)_2$ (E = Sn, Pb), $[NiGe_9]^{3-}$ in $[K(2,2,2\text{-crypt})]_6[Ni@Ge_9]_2 \cdot 3en$, and $[RhIn_9]$ in $EuRh_2In_8$.[16,31]

Adjacent $[CoIn_9]$ cages are interconnected via sharing the trigonal In_3 faces in one-dimensional $[CoIn_6]$ arrays; the latter are further condensed by sharing In(1) vertexes into a $[Co_2In_{11}]$ double cluster chain (Figure 2b). Such connectivity also resulted in the short interchain In(4)−In(4) distance of 3.2131(9) Å. These $[Co_2In_{11}]$ double chains are further bridged by In(5) atoms via In−In bonds (3.1127(7)−3.2431(6) Å) in a complicated 3D framework, forming two types of tunnels along the *c*-axis on the basis of $[In_8]$ eight-membered rings and pentagonal $[In_5]$ five-membered rings, which are occupied by Eu(1) and Eu(2) atoms, respectively (Figure 1a). Eu(1) atom is surrounded by four In(3) and eight In(5) atoms, whereas Eu(2) atom is 11-coordinated by one In(1), two In(2), four In(4), and four In(5) atoms (Figure S1, Supporting Information). The Eu−In distances range from 3.2679(5) to

(24) (a) Madsen, G. K. H.; Blaha, P.; Schwarz, K.; Sjöstedt, E.; Nordström, L. *Phys. Rev. B: Condens. Matter Mater. Phys.* **2001**, *64*, 195134. (b) Schwarz, K.; Blaha, P.; Madsen, G. K. H. *Comput. Phys. Commun.* **2002**, *147*, 71. (c) Perdew, J. P.; Burke, K.; Ernzerhof, M. *Phys. Rev. Lett.* **1996**, *77*, 3865. (d) Blaha, P.; Schwarz, K.; Madsen, G. K. H.; Kvasnicka, D.; Luitz, J. *WIEN2K, An Augmented Plane Wave + Local Orbitals Program for Calculating Crystal Properties*; Karlheinz Schwarz: Techn. Universität Wien, Austria, 2001.

(25) Blöchl, P. E.; Jepsen, O.; Andersen, O. K. *Phys. Rev. B: Condens. Matter Mater. Phys.* **1994**, *49*, 16223.

(26) (a) Jepsen, O.; Andersen, O. K. *The Stuttgart TB-LMTO Program*, Version 4.7. (b) Von Barth, U.; Hedin, L. *J. Phys. C: Solid State Phys.* **1972**, *5*, 1629. (c) Lambrecht, W. R. L.; Andersen, O. K. *Phys. Rev. B: Condens. Matter Mater. Phys.* **1986**, *34*, 2439.

(27) (a) Lambrecht, W. R. L.; Andersen, O. K. *Phys. Rev. B: Condens. Matter Mater. Phys.* **1986**, *34*, 2439. (b) Andersen, O. K. *Phys. Rev. B: Condens. Matter Mater. Phys.* **2000**, *62*, R16219. (c) Tank, R. W. *Phys. Status Solidi B* **2000**, *217*, 89. (d) Pavarini, E. *New J. Phys.* **2005**, *7*, 188.

(28) Pauling, L.; Kamb, B. *Proc. Natl. Acad. Sci. U.S.A.* **1986**, *83*, 3569.

(29) Donohue, J. *The Structures of the Elements*; Wiley: New York, 1974.

(30) (a) Viklund, P.; Lidin, S.; Berastegui, P.; Häussermann, U. *J. Solid State Chem.* **2002**, *164*, 100. (b) Macaluso, R. T.; Sarrao, J. L.; Pagliuso, P. G.; Moreno, N. O.; Goodrich, R. G.; Browne, D. A.; Fronczek, F. R.; Chan, J. Y. *J. Solid State Chem.* **2002**, *166*, 245. (c) Zaremba, V. I.; Rodewald, U. C.; Hoffmann, R.-D.; Kalychak, Y. M.; Pöttgen, R. *Z. Anorg. Allg. Chem.* **2003**, *629*, 1157.

(31) (a) Scharfe, S.; Fässler, T. F.; Stegmaier, S.; Hoffmann, S. D.; Ruhland, K. *Chem.—Eur. J.* **2008**, *14*, 4479. (b) Goicoechea, J. M.; Sevov, S. C. *J. Am. Chem. Soc.* **2006**, *128*, 4155. (c) Ugrinov, A.; Sevov, S. C. *Inorg. Chem.* **2003**, *42*, 5789.

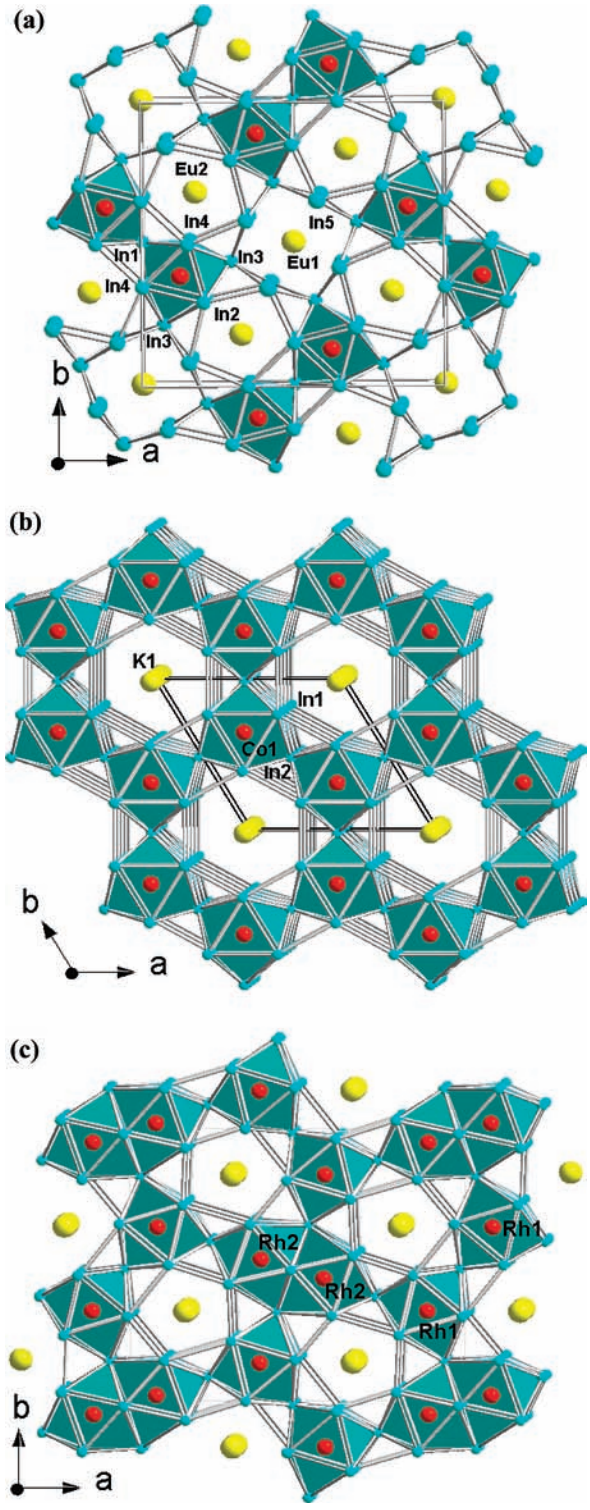

Figure 1. View of the structures of $Eu_3Co_2In_{15}$ (a), KCo_2In_9 (b), and $EuRh_2In_8$ (c) along the *c*-axis. The europium (or potassium), cobalt (or rhodium), and indium atoms are drawn as large yellow, red, and sky-blue spheres, respectively. The M-centered [MIn_9] cluster cage is emphasized with a sky-blue polyhedron.

3.6691(5) Å, which are comparable to those reported in $EuRhIn_2$ and $EuRh_2In_8$.[16]

KM_2In_9 (M = Co, Ni) belongs to the $BaFe_2Al_9$ structure type (Figure 1b).[32] Because the two compounds are isostructural, only the structure of KCo_2In_9 will be discussed in detail as a representative. There are one K, one Co, and two

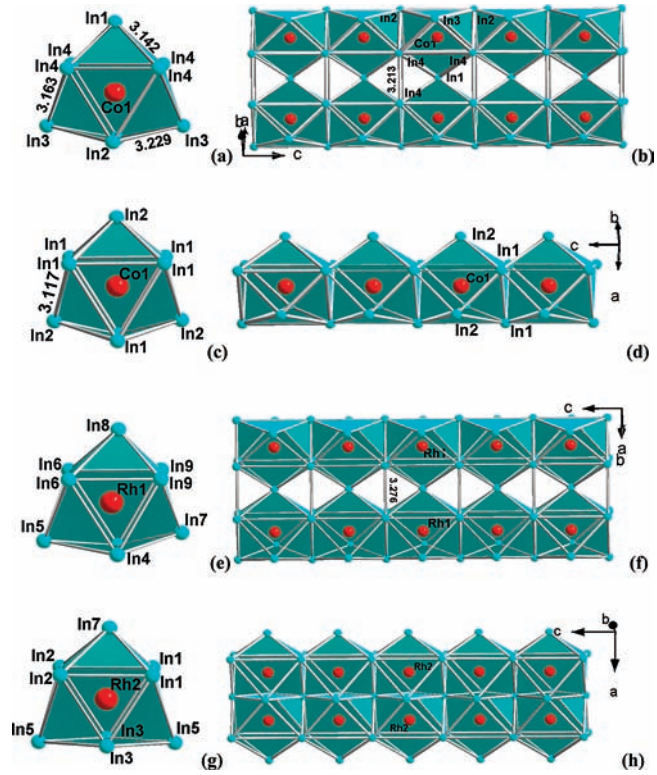

Figure 2. Comparison of the [$CoIn_9$] clusters and various chains in $Eu_3Co_2In_{15}$ (a, b), KCo_2In_9 (c, d), and $EuRh_2In_8$ (e−h).

In sites in the asymmetric unit of KCo_2In_9. The [In_9] cage is formed by six In(1) and three In(2) atoms with a symmetry of D_{3h} (Figure 2c). It should be mentioned that the similar [$RhIn_9$] cluster in $EuRh_2In_8$ with a low symmetry of C_s is much more distorted, compared with [$CoIn_9$] clusters in $Eu_3Co_2In_{15}$ and KCo_2In_9. Differently from that in $Eu_3Co_2In_{15}$, the [$CoIn_6$] chains in KCo_2In_9 are directly interconnected via corner sharing of In(2) atoms and exo In(1)−In(1) bonds in a 3D honeycomb-like [Co_2In_9] framework, forming 1D tunnels along the *c*-axis made by [In_6] six-membered rings (Figure 1b). The intercage In(1)−In(1) distance of 3.1733(4) Å is slightly shorter than that in $Eu_3Co_2In_{15}$ (3.2131(9) Å). The K^+ cations are located at the above tunnels. Each potassium atom is surrounded by 12 indium atoms (K−In 3.8153(3) Å) in a sandwich fashion (Figure S1, Supporting Information).

It is interesting to compare the structure of $Eu_3Co_2In_{15}$ and KCo_2In_9 with $EuRh_2In_8$. In $Eu_3Co_2In_{15}$, [Co_2In_{11}] double cluster chains are interconnected by isolated indium atoms, whereas in KCo_2In_9, the [$CoIn_6$] single cluster chains are directly interconnected via corner sharing and exobonds. The structure of $EuRh_2In_8$ with a $CaCo_2Al_8$ type contains two types of double cluster chains.[16] The first one is similar to that in $Eu_3Co_2In_{15}$ (Figure 2e,f), whereas the second type is formed by [$RhIn_9$] cages interconnected via face sharing (Figure 2g,h). Two such different double chains in a 1:1 ratio in $EuRh_2In_8$ are interconnected via corner sharing into a 3D framework, forming 1D channels based on [In_5] rings which are occupied by Eu atoms (Figure 1c).

(32) Turban, K.; Schäfer, H. *J. Less−Common Met.* **1975**, *40*, 91.

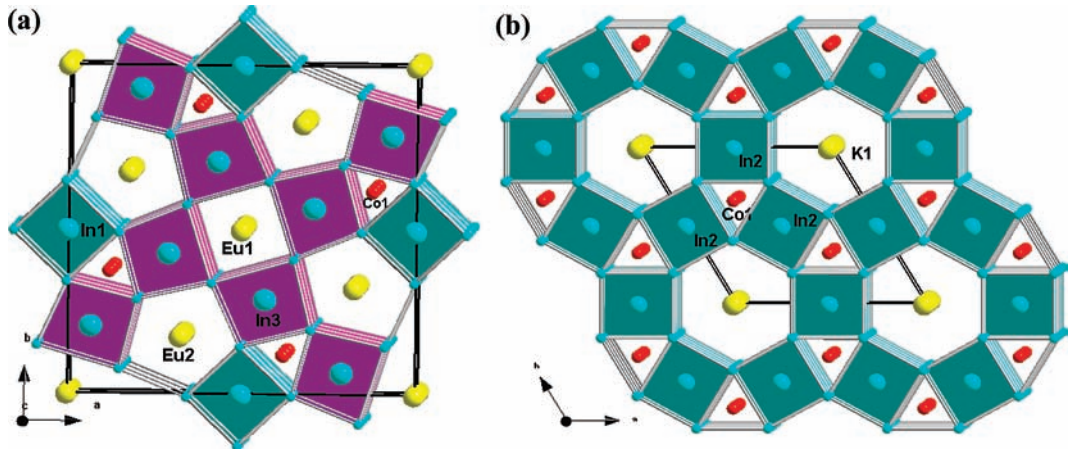

Figure 3. Perspective view of $Eu_3Co_2In_{15}$ (a) and KCo_2In_9 (b) based on the bcc-like indium cubes.

The most prominent feature for $Eu_3Co_2In_{15}$ and KCo_2In_9 is the stacking manner of slightly distorted bcc-like indium cubes, which is reminiscent of the structure of elemental indium (*I*4/*mmm*).[29] In $Eu_3Co_2In_{15}$, five crystallographically independent indium sites are all situated in slightly distorted cube-like indium polyhedra, of which the In(1), In(2), In(3), and In(4) atoms are augmented by additional neighbors of Co(1) atoms, whereas the In(5) atom with a similar coordination environment is not in contact with Co(1) atoms (In(5)···In(5) = 3.670 Å; Figure S2, Supporting Information). The cubic polyhedra centered with In(1) and In(3) atoms are interconnected via face and vertex sharing to form a 3D framework with three types of channels: trigonal, square, and pentagonal, which are filled by Co(1), Eu(1), and Eu(2) atoms, respectively (Figure 3a). In KCo_2In_9, the close packing of cubic polyhedra centered with In(2) atoms constructs the 3D framework, forming two types of channels, trigonal and hexagonal, which are filled by Co(1) and K(1) atoms, respectively (Figure 3b). Distorted bcc-like indium cubes are the basic building blocks of a variety of binary indium-rich compounds MIn_3 (M = Co, Rh, Ir)[33] as well as the ternary indium rich intermetallic phases, for example, $CaMIn_4$ (M = Rh, Ir),[20] $EuRh_2In_8$,[16] $REMIn_5$, and RE_2MIn_8 (M = Co, Rh, Ir).[17,34] It is interesting to note that the stacking manner of the indium cubic greatly depends on the content of indium metal. Greater indium content will lead to much more closer stacking of indium cubes.

Band Structure Calculations. To further investigate the nature of the bond character and transport property of $Eu_3Co_2In_{15}$, we carried out highly accurate band structure calculations by using the FPLAPW method. It is seen that the valence band crosses the Fermi level with no visible band gap from the band structure, which means that $Eu_3Co_2In_{15}$ exhibits metallic character (Figure S3, Supporting Information). The spin polarization was properly taken into account by considering the unpaired f-electron effect of the europium ion. The calculated total density of states (TDOS) and the partial density of states (PDOS) from each element are given in Figure 4. Two narrow peaks observed below and above the Fermi level for spin up and down, respectively, belong to the Eu 4f states. The states with spin up are occupied while the states with spin down are empty. The existence of spin splitting only for Eu 4f orbitals indicates that the magnetic moment of $Eu_3Co_2In_{15}$ is localized almost entirely at the europium cations. The calculation converges to theoretical saturation moments of 6.944 and 7.134 μ_B for the Eu(1) and Eu(2) atoms, respectively, which compares not too badly with the effective moment of 7.94 μ_B for free Eu^{2+}. Hence europium cations are most possibly in +2 oxidation states. The Co 3d bands are mostly localized in the range of −3 to 0 eV. It is noted that the strong In/p−Co/d hybridization just below the Fermi level indicates the strong covalent character of the Co−In bonds. The PDOS of all the indium atoms spreads over the whole energy range (5s, −10 to −3 eV; 5p, −3 to 0 eV) with larger dispersion, which is mostly dominated by the σ interactions between nearly free electron-like In 5p orbitals (Figure 4).

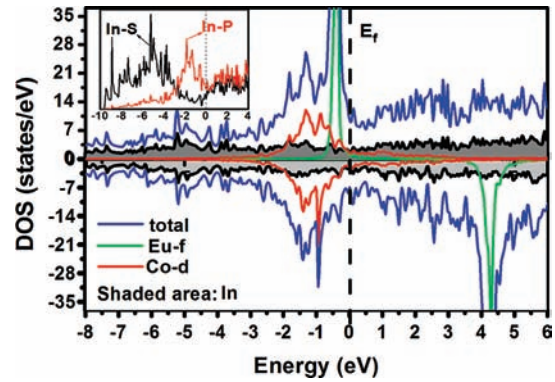

Figure 4. TDOS and PDOS for $Eu_3Co_2In_{15}$. The TDOS (blue solid line), Eu f orbitals (green), Co d orbitals (red), and In (gray shaded area). The Fermi level is set at 0 eV. Inset: specific PDOS for In s and In p.

Band structure calculations for KM_2In_9 (M = Co, Ni) indicate that both compounds are metallic with no visible band gap (Figure S4, Supporting Information). The calculated TDOS and PDOS for the two compounds are given in Figure 5. No spin splitting was observed. In the DOS curve, the states in the energy range of −10 ∼ −4 eV are essentially dominated by In 5s electrons, and the states just below the Fermi level (−3 ∼ −1 eV) are mainly contributed by In 5p

(33) (a) Pöttgen, R.; Hoffmann, R.-D.; Kotayba, G. *Z. Anorg. Allg. Chem.* **1998**, *624*, 244. (b) Pöttgen, R. *J. Alloys Compd.* **1995**, *226*, 59.
(34) Kalychak, Y. M.; Zaremba, V. I.; Baranyak, V. *Izv. Akad. Nauk Ukr.* **1989**, *1*, 209.

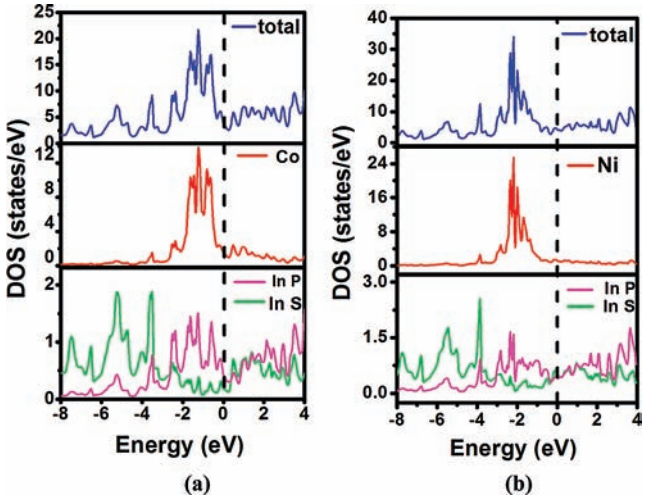

Figure 5. TDOS and PDOS for (a) KCo_2In_9 and (b) KNi_2In_9. The TDOS (blue solid line), Co (Ni) d orbitals (red), In s (green), and In p (purple). The Fermi level is set at 0 eV.

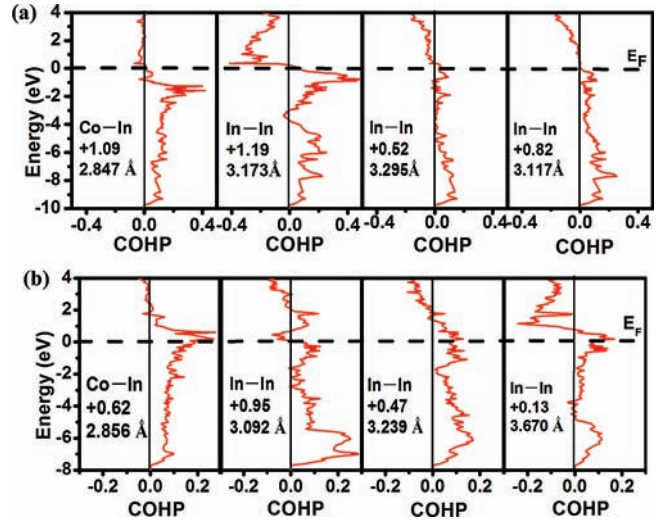

Figure 6. Selected -COHP curves for KCo_2In_9 (a) and $Eu_3Co_2In_{15}$ (b). The integrated values for the overlap -ICOHP per bond up to the Fermi level (dotted line) and the corresponding distances are given.

and Co 3d electrons. For the cobalt site, the symmetrical $[In_9]$ cluster (D_{3h}) decomposes five Co 3d orbitals into a nondegenerate $z^2 - r^2$, doubly degenerate $\{x^2 - y^2, xy\}$, and doubly degenerate $\{xz, yz\}$, whereas the Co 3d band remains as five nondegenerate orbitals in $Eu_3Co_2In_{15}$. The distinct splitting characters of Co 3d orbitals for KCo_2In_9 and $Eu_3Co_2In_{15}$ originate from the different symmetries of $[In_9]$ clusters. In addition, most of the density of 4s states for the K atoms is located just above the Fermi level, which shows that the K atoms transfer their valence electrons to the anionic framework.

The electronic band structure of KNi_2In_9 is similar to that of KCo_2In_9 except for the PDOS of Ni 3d moving toward the lower energy level in KNi_2In_9. It is interesting to compare the electronic structures around the centering transition metal atoms of $[NiIn_{10}]$ clusters in $K_{10}NiIn_{10}$ and $[NiIn_9]$ clusters in KNi_2In_9. For $K_{10}NiIn_{10}$, it is reported that the Ni 3d orbitals remain unperturbed without mixing with indium orbitals.[21c] A similar conclusion regarding inertness of the Ni 3d orbitals has been deduced for several Ni-centered germanium clusters.[35] However, the Ni 3d orbitals in the smaller $[In_9]$ cluster lie on higher energy and strongly hybridize with In 5p orbitals just below Fermi level.

GGA + U (on-site Coulombic energy correction) type calculations for all three compounds were also performed to further understand their electronic structures. It is found that the density of states is unchanged except for small quantitative changes for $Eu_3Co_2In_{15}$ (Figure S5, Supporting Information) and KM_2In_9 (M = Co, Ni; Figure S6, Supporting Information). Namely, the U parameter does not influence the energy and DOS of both 3d and 4f electrons. The calculated spin magnetic moments of 6.944 and 7.134 μ_B for the Eu(1) and Eu(2) atoms are almost unchanged with the U parameter. Thus, the GGA exchange correlation formation can give sufficient and reliable results.

To further check the chemical bonding, the results of the LMTO-ASA calculations have been utilized for the interpretation of bonding through crystal orbital Hamilton population analyses (-COHP), as the WIEN2K code does not support such an analysis (Figure 6).[36] To quantify the interaction between atoms, integrated -COHP (-ICOHP) analyses were also determined, and the calculated values are listed in Tables S2 and S3 of Supporting Information, respectively. Because of the similar chemical bonds of KNi_2In_9 and KCo_2In_9, the bonding character will be described in terms of KCo_2In_9. In KCo_2In_9, both Co−In bonds are effectively optimized at the Fermi level, whereas some Co−In bonding states remained above the Fermi level in $Eu_3Co_2In_{15}$. The Co−In bonds with large -ICOHP of 1.09−1.8 and 0.62−1.01 (eV/bond) for KCo_2In_9 and $Eu_3Co_2In_{15}$, respectively, are significantly bonding. The In−In contacts show various interesting bonding characters depending on the different bond distances. The shorter In−In bonds of 3.1175(2)−3.1733(4) Å for KCo_2In_9 and 3.0920(7) Å for $Eu_3Co_2In_{15}$, respectively, are effectively optimized at the Fermi level with large -ICOHP, whereas the antibonding of In−In states remain partially filled above the Fermi level for longer In−In bonds (3.2952(6) Å in KCo_2In_9 and 3.113−3.243 Å in $Eu_3Co_2In_{15}$, respectively), as shown in Figure 6. It should be noted that partial filling of antibonding In−In states leads to greater In−In bonds, which have been investigated in detail elsewhere.[19] In $Eu_3Co_2In_{15}$, the In−In bonds (3.113−3.243 Å) with -ICOHP in the range of 0.53−0.82 eV/bond are significantly bonding. The -ICOHP value (0.13 eV) for the long In(5)−In(5) distance (3.670 Å) is especially small, as expected, indicating that such a bond is much weaker than those in the $[CoIn_9]$ cluster. The Eu−In bonds (3.268−3.438 Å) are weakly bonding with an average -ICOHP value of about 0.22 eV/bond. The K−In bonds (3.815 Å) with a very small -ICOHP value of 0.07 eV are essentially nonbonding.

In summary, we have successfully obtained a series of novel ternary indides, namely, $Eu_3Co_2In_{15}$ and KM_2In_9 (M = Co, Ni). They all feature a 3D network based on 1D $[MIn_6]$ single cluster chains assembled by transition metal centered $[In_9]$ cages. Furthermore, they are also in line with the known

(35) Goicoechea, J. M.; Sevov, S. C. *Angew. Chem., Int. Ed.* **2005**, *44*, 4026.

indium-rich compounds with the common structural motifs of the distorted bcc-like indium cubes. These compounds further illustrate the effect of cations on the structure type formed. Because of the lack of the single phases of these compounds, unfortunately, we cannot measure their magnetic or electric properties.

Acknowledgment. We thank the National Nature Science Foundation of China (Nos. 20573113, 20825104, and 20521101) for its financial support.

Supporting Information Available: Tables of anisotropic displacement parameters, selected bond lengths and the corresponding -ICOHP values, figures showing the coordination geometries around Eu, K, and all In atoms, calculated DOS based on GGA + U type calculation and band structures for all compounds, and X-ray crystallographic files for three compounds in CIF format. This material is available free of charge via the Internet at http://pubs.acs.org.

IC8019765

(36) (a) Mudring, A.-V.; Corbett, J. D. *J. Am. Chem. Soc.* **2004**, *126*, 5277. (b) Bobev, S.; Bauer, E. D.; Thompson, J. D.; Sarrao, J. L.; Miller, G. J.; Eck, B.; Dronskowski, R. *J. Solid State Chem.* **2004**, *177*, 3545.